JOURNAL OF VIROLOGY, July 2005, p. 8909–8919 Vol. 79, No. 14
0022-538X/05/$08.00+0 doi:10.1128/JVI.79.14.8909–8919.2005

In Vivo Self-Interaction of Nodavirus RNA Replicase Protein A Revealed by Fluorescence Resonance Energy Transfer

Billy T. Dye,[1,2] David J. Miller,[2]† and Paul Ahlquist[1,2]*

Howard Hughes Medical Institute[1] and Institute for Molecular Virology,[2] University of Wisconsin, Madison, Wisconsin 53706

Received 21 January 2005/Accepted 29 March 2005

Flock house virus (FHV) is the best-characterized member of the *Nodaviridae*, a family of small, positive-strand RNA viruses. Unlike most RNA viruses, FHV encodes only a single polypeptide, protein A, that is required for RNA replication. Protein A contains a C-proximal RNA-dependent RNA polymerase domain and localizes via an N-terminal transmembrane domain to the outer mitochondrial membrane, where FHV RNA replication takes place in association with invaginations referred to as spherules. We demonstrate here that protein A self-interacts in vivo by using flow cytometric analysis of fluorescence resonance energy transfer (FRET), spectrofluorometric analysis of bioluminescence resonance energy transfer, and coimmunoprecipitation. Several nonoverlapping protein A sequences were able to independently direct protein-protein interaction, including an N-terminal region previously shown to be sufficient for localization to the outer mitochondrial membrane (D. J. Miller and P. Ahlquist, J. Virol. 76:9856–9867, 2000). Mutations in protein A that diminished FRET also diminished FHV RNA replication, a finding consistent with an important role for protein A self-interaction in FHV RNA synthesis. Thus, the results imply that FHV protein A functions as a multimer rather than as a monomer at one or more steps in RNA replication.

Flock house virus (FHV) is an alphanodavirus with a 4.5-kb positive-strand RNA genome. In addition to its natural host, the grass grub *Costelytra zealandica* (66), FHV can replicate in *Drosophila* (12), mosquito (11), *Spodoptera* (30), mammalian (6), plant (67), and yeast (*Saccharomyces cerevisiae*) (51) cells upon the introduction of its genome by transfection or by transcription from DNA vectors. The genetic simplicity and wide host range of FHV have made it an attractive model for the study of replication complex assembly (39, 40), RNA replication (27, 34), viral RNA encapsidation (63, 64, 77), and virion structure (18, 30, 61, 62, 69).

The FHV genome consists of two nonpolyadenylated RNAs, RNA1 and RNA2 (8). RNA1 encodes protein A, a 112-kDa protein with an RNA-dependent RNA polymerase (RdRp) domain and other sequences that are essential for RNA replication. In addition, sequence at the 3′ end of RNA1 that partially overlaps the protein A open reading frame (ORF) encodes a subgenomic transcript, RNA3. RNA3 encodes B2, a suppressor of silencing that is required for the continued accumulation of replicating FHV RNA in insect and mammalian cells (7, 33). B2 is expressed only from RNA3 and is not translated directly from genomic RNA1. RNA2 encodes the coat protein precursor, α, which is cleaved into β and γ subunits upon virion maturation (64).

Protein A replicates the FHV genome by synthesizing negative-sense copies of both RNA1 and RNA2 that, in turn, are used as templates for the synthesis of a nonstoichiometric excess of positive-sense copies. Protein A also synthesizes negative- and positive-sense transcripts of subgenomic RNA3, which it can also replicate independently of RNA1 (15). Interestingly, RNA3 transcription is necessary for, yet inhibited by, RNA2 replication (3, 15, 16, 78). Thus, the activity of protein A in genomic and subgenomic RNA synthesis is modulated to coordinate the successive production and levels of synthesis of various FHV RNA species.

Protein A is directed to the outer mitochondrial membrane by an N-terminal region containing a 19-amino-acid transmembrane domain (38). Electron microscopy has revealed that FHV replication takes place in association with invaginations of the outer mitochondrial membrane referred to as spherules (39). The replication complexes of many other positive-strand RNA viruses have been shown to form similar structures on host membranes, although the specific membrane that is used varies from virus to virus (for examples, see references 31, 58–60, and 72).

Most positive-strand RNA viruses typically encode multiple factors required for RNA replication, expressed either from discrete ORFs (1, 44, 45), by proteolytic cleavage of a single polyprotein (43, 54), or by readthrough translation (49, 56). Although some RdRps have polymerase activity as individual proteins, they still require additional viral polypeptides for complete functionality (4, 5, 32, 35, 36, 45, 48). In addition, individual subunits of the replication factors from many viruses have been shown to oligomerize, adding even more complexity to their replication machinery (9, 21, 41, 46, 52, 74).

In contrast to the examples given above, protein A is the only virus-encoded protein that is required for FHV RNA replication, yet it performs multiple roles in the FHV life cycle and replicates multiple forms of viral RNA (7, 28, 50). The complexities and interactions of other RNA virus replicase proteins suggest that protein A might function as a multimer

* Corresponding author. Mailing address: Institute for Molecular Virology, University of Wisconsin-Madison, 1525 Linden Dr., Madison, WI 53706. Phone: (608) 263-5916. Fax: (608) 265-9214. E-mail: ahlquist@facstaff.wisc.edu

† Present address: Division of Infectious Diseases, Department of Medicine, University of Michigan Medical School, Ann Arbor, Michigan.

for at least some RNA replication steps. To test for possible self-association of protein A, we performed fluorescence resonance energy transfer (FRET), bioluminescence resonance energy transfer (BRET), and coimmunoprecipitation experiments. Each of these independent approaches indicated that protein A self-interacts. To further characterize this interaction, we identified several protein A sequences that were sufficient to direct homotypic protein interactions as assayed by FRET. Furthermore, mutations in protein A that decreased FRET also decreased FHV RNA replication in vivo, implying that protein A self-interaction is functionally important for RNA replication.

MATERIALS AND METHODS

Plasmids. All yeast protein expression plasmids described in the present study are low-copy, centromeric vectors that express their respective encoded sequences under the galactose-inducible *GAL1* promoter. Transcription of these constructs is terminated by the *ADH1* terminator and polyadenylation sequence. All yellow fluorescent protein (YFP) fusion constructs contain the *LEU2* selectable marker; all cyan fluorescent protein (CFP) and *Renilla* luciferase fusion constructs contain *HIS3*.

Plasmids pA-YFP and pA-CFP express full-length, FHV protein A with a C-terminal fusion to a 4-amino-acid linker (GGSG) and either YFP or CFP and were derived from pFA-C/HA and pFA-C/HA(HIS), respectively, which each contain full-length protein A fused to an 8-amino-acid linker (GGSGGSGG), followed by the hemagglutinin (HA) tag. Primers 5′-GCTAGCTCAGCCACA ACCATCTAACAACAGAAAGGGTGGTTCCGGAGGTTCTGGTGG-3′ and 5′-ACCGCTCGAGTCAAGCGTAGTCTGGGACGTCGTATGGGTAACCAC CAGAACCTCCGG-3′, which encode the HA tag, were annealed, extended by PCR, and cloned into pGEM3 as a BlpI/XhoI fragment to create pGEM/link/cyc. A BlpI/HindIII fragment from pGEM/link/cyc was then subcloned into pFA (40) to create pFA-C/HA. An EcoRI/AlwNI fragment from pGEM/link/cyc was subcloned into pRS313 (GenBank accession number U03439) to generate pFA-C/HA(HIS), which contains *HIS3* rather than *LEU2* as in pFA-C/HA. Subsequently, pA-YFP was generated by PCR amplifying the ORF of YFP from pYFP/GAL (14) using the primers 5′-GCTCCGGAATGTCTAAAGGTGAAGAATTATTC-3′ and 5′-CGG GATCCGACGTCTTATTTGTACAATTCATCC-3′ and inserting the product into pFA-C/HA as a BspEI/AatII fragment. Plasmid pA-CFP was generated by PCR amplifying the enhanced CFP ORF from pECFP-N1 (BD Biosciences Clontech, Palo Alto, CA) using the primers 5′-GCTCCGGAATGGTGAGCAAGGGCGAG GAGC-3′ and 5′-GCGACGTCTTACTTGTACAGCTCGTCCATG-3′ and inserting the product into pFA-C/HA(His) as a BspEI/AatII fragment.

Protein A-YFP deletion constructs were created by PCR amplifying the indicated regions of the protein A ORF with pFA as a template and primer pairs that add a PstI site to the 5′ end of the amplified region and a BspEI site to the 3′ end. These PCR products were then cloned as PstI/BspEI fragments into pA-YFP, replacing the full-length protein A ORF. Counterpart CFP fusion plasmids were made by subcloning XbaI/BspEI fragments from each YFP deletion construct into pA-CFP. In all deletion constructs, the C terminus of the protein A sequence is fused to YFP or CFP via an intervening 4-amino-acid linker (GGSG).

Protein A-YFP constructs containing point mutations are identical to pA-YFP except that the codon for the indicated amino acid was changed to encode alanine rather than the wild-type (wt) residue. These mutants were cloned by using a multistep PCR method. Three separate PCRs were performed such that PCR1 generated a 5′ portion of a mutant, PCR2 generated a 3′ portion, and PCR3 united the two portions. For each mutant, PCR1 contained pFA as a template, a sense primer corresponding to the 5′ end of the wt protein A ORF, and an antisense primer containing the indicated mutation and ~35 nt of wt protein A sequence flanking each side of the mutated sequence. PCR2 contained pFA as a template, a sense primer complementary to the respective mutagenic primer used in PCR1, and an antisense primer corresponding to codons 494 to 500 of the wt protein A ORF. In PCR3, the products of PCR1 and PCR2 were combined and amplified by using the sense primer from PCR1 and the antisense primer from PCR2. The product of PCR3 was then cloned as a PstI/BglII fragment into pA-YFP.

Plasmid pA-RL expresses full-length, FHV protein A containing a C-terminal fusion to a 4-amino-acid linker (GGSG) and *Renilla reniformis* luciferase (RL). The ORF of RL was PCR amplified by using pRL-TK (Promega, Madison, WI) as a template and primers 5′-GCTCCGGAATGACTTCGAAAGTTTATGAT CC-3′ and 5′-CGGGATCCGACGTCTTATTGTTCATTTTTGAGAAC-3′ and inserted into pFA-C/HA(His) as a BspEI/AatII fragment.

Plasmids used in *Drosophila* S2 cells derive from pMT/V5-HisA (Invitrogen, Carlsbad, CA). Each expresses a protein A message transcribed by the *Drosophila* metallothionein promoter, terminated by the simian virus 40 polyadenylaton signal, and translated from the EMCV IRES. The wild-type (untagged) protein A plasmid pDJM11 was generated by inserting the Acc65I/XhoI fragment from pBDL300 (a protein A construct containing the EMCV IRES in the 5′ untranslated region) into pMT/V5-HisA. Plasmids pA-HA (containing the HA tag) and pA-His_6 (containing the His_6 tag) were generated by placing the BglII/XhoI fragment from pFA-C/HA or pFA-C/H6 into pDJM11, respectively. Plasmid pFA-C/H6 was cloned in the same manner as pFA-C/HA, except that the primers 5′-GCTAGCTCAGCCACAACCATCTAACAACAGAAAGGGTGGTTC CGGAGGTTC-3′ and 5′-ACCGCTCGAGTCAGTGGTGGTGGTGGTGGT GACCACCAGAACCTCCGGAACCA-3′, which encode the His_6 tag, were used. Plasmid pCoBlast (Invitrogen) expresses the blasticidin resistance gene under the copia long terminal repeat promoter.

The FHV replication reporter plasmid pFHV1-RL expresses a replication-competent FHV RNA1 transcript that contains a frameshift mutation in the protein A ORF such that replication is dependent on the expression of a protein A message in *trans*. Plasmid pFHV1-RL also contains the complete ORF of *Renilla* luciferase, which was inserted into the region of RNA1 encoding the subgenomic RNA3. Since RNA3 is produced only upon the replication of RNA1 by protein A but not as a primary transcript of the plasmid, RL is expressed only if protein A-dependent RNA replication occurs. Thus, when pFHV1-RL is cotransformed with a plasmid expressing protein A, luciferase activity can be measured as a reporter for protein A activity. Plasmid pFHV1-RL was constructed by first placing a multiple cloning site into pF1fs (50) immediately upstream of the B2 ORF by inserting a multistep PCR product as a Bsp120I/BlpI restriction fragment. The PCR product was generated by first amplifying pF1 (50) with the primers 5′-GGATCCCTCGAGGCCTAGGTAACCGTCGACCG CGGCGCCTCTAGATTAAACGATGCCAAGCAAAC-3′ and 5′-TTTCGGG CTAGAACGGGTGT-3′ in PCR1 and with the primers 5′-GCGGGATCCTC AACGCTAGGCTTATCGGTATG-3′ and 5′-AAAGGTTTTAACCGGAAGT AAGAGCAGCAAGAAGCACTAGCAATG-3′ in PCR2 and then combining PCR1 and PCR2 and reamplifying them with the primers 5′-GCGGGATCCT CAACGCTAGGCTTATCGGTATG-3′ and 5′-TTTCGGGCTAGAACGGGT GT-3′. Second, the *Renilla* luciferase ORF was cloned into the multiple cloning site as an XhoI/XbaI fragment from pDK502. (The *Renilla* luciferase ORF was first cloned into pDK502 as an EcoRI/SalI fragment produced from the PCR amplification of pRL-Null [Promega, Madison, WI] with the primers 5′-CGGA ATTCAGGCCTCTCGAGAATATAATGACTTCGAAAGTTTATGATCCA-3′ and 5′-TTCCGGGTCGACGTTAACGGTAACCTTATTGTTCATTTTTGAG AACTCG-3′.) Third, an MluI/BsrGI restriction fragment was substituted for that from pBDL46 to change the selectable marker from *TRP1* to *HIS3*. Fourth, the start codon of the B1 ORF was disrupted by substituting the Bsp120I/XhoI fragment for a PCR product generated by amplifying pF1fs with the primers 5′-GCGGGATCCTCAACGCTAGGCTTATCGGTATG-3′ and 5′-CGTTTAA CTCGAGATTGGTAACGATTCGTC-3′.

Yeast strains and transformations. *Saccharomyces cerevisiae* strain BY4743 (*his3Δ1 leu2Δ0 ura3Δ0*) was transformed with the indicated plasmids by the LiAc/PEG method (17), and plasmids were maintained by constant selection for their respective auxotrophic markers.

Flow cytometry. Flow cytometry was performed as previously described (14). In brief, yeast cells were grown 1 to 2 days in minimal selective media containing galactose, passed through a 0.45-μm-pore-size filter, and diluted in phosphate-buffered saline (PBS; 1 mM KH_2PO_4, 3 mM Na_2HPO_4, 155 mM NaCl [pH 7.5]) containing propidium iodide. Flow cytometry data were collected with a multi-laser FACSVantage SE flow cytometer (Becton Dickinson, San Jose, CA) equipped with two water-cooled lasers: an argon Innova 90, tuned to 488 nm at 100 mW, and an Innova 302C krypton laser, tuned to 413 nm at 200 mW (both from Coherent, Santa Clara, CA). Propidium iodide was excited with the 488-nm laser line, and its fluorescence was measured by using a 630/30 band-pass filter. YFP was excited with the 488-nm laser line, and its fluorescence was measured by using a 546/10 band-pass filter. The 413-nm laser line was used to excite CFP, and the CFP fluorescence was separated from the FRET channel with a 505-nm short-pass dichroic mirror. The FRET channel was measured by using a 550/30-nm band-pass filter, whereas the CFP fluorescence was measured by using a 470/20-nm band-pass filter. The spectral overlap was calculated for each fluorescence emission and set by using single-color controls. The data were collected from 30,000 cells from each yeast culture. All data were acquired by using the FACSDiVa digital electronics and software package (Becton Dickinson, San Jose, CA), and all analyses of these data were performed by using FlowJo (Tree

Star, Inc., Ashland, OR). Live cells were identified as those that did not exhibit propidium iodide uptake. Only data from live cells were used in analyses. All fluorescence measurements are reported as the relative fluorescence intensity.

BRET assay. Yeast cultures transformed with the indicated plasmids were grown at 26°C for 2 days in minimal selective medium containing galactose, and cells were collected by low-speed centrifugation and resuspended in PBS. Immediately after the addition of coelenterazine (Biotium, Hayward, CA) to a final concentration of 10 μM, yeast cells were assayed for BRET by monitoring the light emitted between 450 and 570 nm with a PTI QuantaMaster Model C-60/2000 spectrofluorometer (Photon Technology International, Lawrenceville, NJ) in the absence of an excitation laser. As a reference, direct YFP fluorescence was observed by monitoring the light emitted between 515 and 570 nm while cultures were excited with 475-nm light prior to the addition of coelenterazine.

***Drosophila* cell culture, transfection, and selection of stable lines.** *Drosophila melanogaster* S2 cells (Invitrogen) were grown at 28°C in complete medium (Schneider's *Drosophila* medium containing 1 U of penicillin/ml, 1 μg of streptomycin/ml, and 10% heat-inactivated fetal bovine serum; all from Invitrogen, Carlsbad, CA). Cells were seeded at a density of 5×10^5 cells per well in 12-well tissue culture plates and then grown overnight prior to transfection. Cells were cotransfected with 10 μg of the indicated expression plasmid and 0.5 μg of the selection plasmid, pCoBlast (Invitrogen), by lipid-mediated transfection with Cellfectin (Invitrogen) according to the manufacturer's instructions. Cells were transfected for 4 h in serum-free medium. The cells were incubated for an additional 18 to 20 h after supplementation with an equal volume of complete medium. The transfection medium was then replaced with complete medium containing 25 μg of blasticidin/ml. Cells were transferred into new media after ca. 7 to 10 days, at which time resistant cells began to proliferate. Cells were subsequently passaged in fresh selection medium every 4 to 6 days for at least three passages, and aliquots were frozen for storage in liquid nitrogen. The cells used in immunoprecipitation experiments were stably transfected, heterogeneous populations and were maintained under continuous selection.

Coimmunoprecipitation. Stably transfected *Drosophila* S2 cells were induced to express the indicated, epitope-tagged protein A species by the addition of 0.5 mM $CuSO_4$ to the culture medium. At 24 h after induction, cells were harvested, washed with ice-cold Tris-buffered saline (TBS; 50 mM Tris [pH 7.6], 100 mM NaCl), and lysed for 30 min on ice in TBS containing 1% (vol/vol) Triton X-100 and protease inhibitor cocktail (P2714; Sigma-Aldrich, St. Louis, MO). Lysates were centrifuged for 5 min at $500 \times g$ to remove nuclei and large debris and then precleared by incubation with agarose beads coupled to goat anti-mouse immunoglobulin G (IgG) for 1 h at 4°C with gentle rotation. Precleared lysates were incubated overnight at 4°C with gentle rotation in the presence of either agarose beads coupled to mouse anti-HA monoclonal antibody (PA2095, Sigma-Aldrich) or, as a control, agarose beads coupled to mouse anti-FLAG monoclonal antibody A2220 (Sigma-Aldrich). Immunoprecipitates were collected by centrifugation at $10{,}000 \times g$ for 1 min and washed four times with TBS containing 1% Triton X-100. Samples were then separated by sodium dodecyl sulfate-polyacrylamide gel electrophoresis, transferred to polyvinylidene difluoride membrane, and immunoblotted with rabbit anti-HA IgG or rabbit anti-His_6 IgG (both from Santa Cruz Biotech, Santa Cruz, CA).

FHV RNA replication assay. Yeast cells were cotransformed with the indicated protein A-YFP fusion construct and pFHV1-RL and were grown at 26°C in selective media containing galactose for a total of 3 days. Cultures were diluted into fresh media to a starting optical density at 600 nm of 0.075 each day to maintain growth in log phase. Cells were collected by centrifugation and resuspended in PBS, and the cell density was measured as the optical density at 600 nm. Aliquots (50 μl) of the resuspended cultures were assayed for *Renilla* luciferase activity in a 96-well MicroLumat Plus luminometer (Perkin-Elmer, Boston, MA) over 10-s read times that followed the injection of coelenterazine (Biotium, Hayward, CA) to a final concentration of 1 μM. Luciferase activity was measured as relative luminescence units and normalized to the cell density and protein A-YFP expression (measured as the geometric mean YFP fluorescence) of each sample.

RESULTS

Self-interaction of protein A. (i) FRET. To investigate protein A self-interaction, we tested whether FRET was produced upon the coexpression of protein A-CFP (A-CFP) and protein A-YFP (A-YFP) fusion proteins in yeast cells (Fig. 1). The respective fluorescent protein was fused to the C terminus of full-length, wt protein A to retain replication activity, as shown below. In this system, FRET occurs if light energy is transferred from A-CFP to A-YFP, producing YFP fluorescence upon the excitation of CFP. The efficiency of FRET is inversely proportional to the sixth power of the distance between chromophores (19). Thus, FRET can occur only if the chromophores in the two fusion proteins are positioned very close to one another. The distance at which energy transfer reaches 50% efficiency is defined as the Förster radius, which for a CFP/YFP pair is ~50 Å, as measured from the chromophores located in the center of each protein (47). Given the ~15 Å radii of CFP and YFP, this corresponds to a distance of only ~20 Å between the proteins. If CFP and YFP are separated by little more than twice their Förster radius (a distance of only ~100 Å between chromophores or ~70 Å between the proteins), FRET will diminish to a point indistinguishable from background. The close proximity required for FRET is unlikely to be achieved except by stable physical interaction between the two fusion proteins and, accordingly, FRET has been demonstrated to be a reliable indicator of steady-state protein-protein interaction (13, 14, 23, 70).

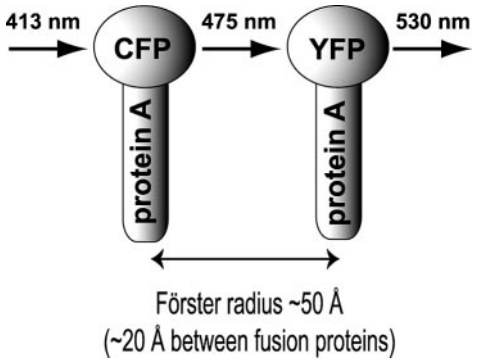

FIG. 1. Design of FRET experiments. FRET occurs when light energy is transferred from a protein A-CFP fusion to a protein A-YFP fusion. FRET is possible only if the chromophores in the respective fusion proteins are within very close proximity and are properly juxtaposed. The Förster radius is the distance between chromophores at which FRET occurs at 50% efficiency and is ca. 50 Å for a CFP/YFP pair. Considering the radii of the barrel–shaped structures that surround their chromophores, a pair of CFP and YFP fusion proteins positioned at their Förster radius would be separated by only 20 Å. As discussed in the text, such close association is normally achieved only upon the interaction of the protein A sequences fused to each. FRET has been demonstrated to be a reliable indicator of steady-state protein-protein interaction (13, 14, 23, 70).

Yeast were cotransformed with either pA-CFP and pA-YFP, which direct the expression of the respective protein A fusion proteins under the galactose-inducible *GAL1* promoter, or with pA-CFP and pYFP, a plasmid which expresses free YFP without any additional sequences. After growth in galactose-containing media to induce protein expression, the fluorescence properties of 30,000 yeast cells from each sample were analyzed by flow cytometry. Since free YFP was not expected to interact with the A-CFP fusion protein, their coexpression served as a negative control. Protein-protein interaction was thus tested by determining whether cells in the experimental sample coexpressing A-CFP and A-YFP had significantly higher FRET intensities than cells in the negative control sample coexpressing A-CFP and YFP.

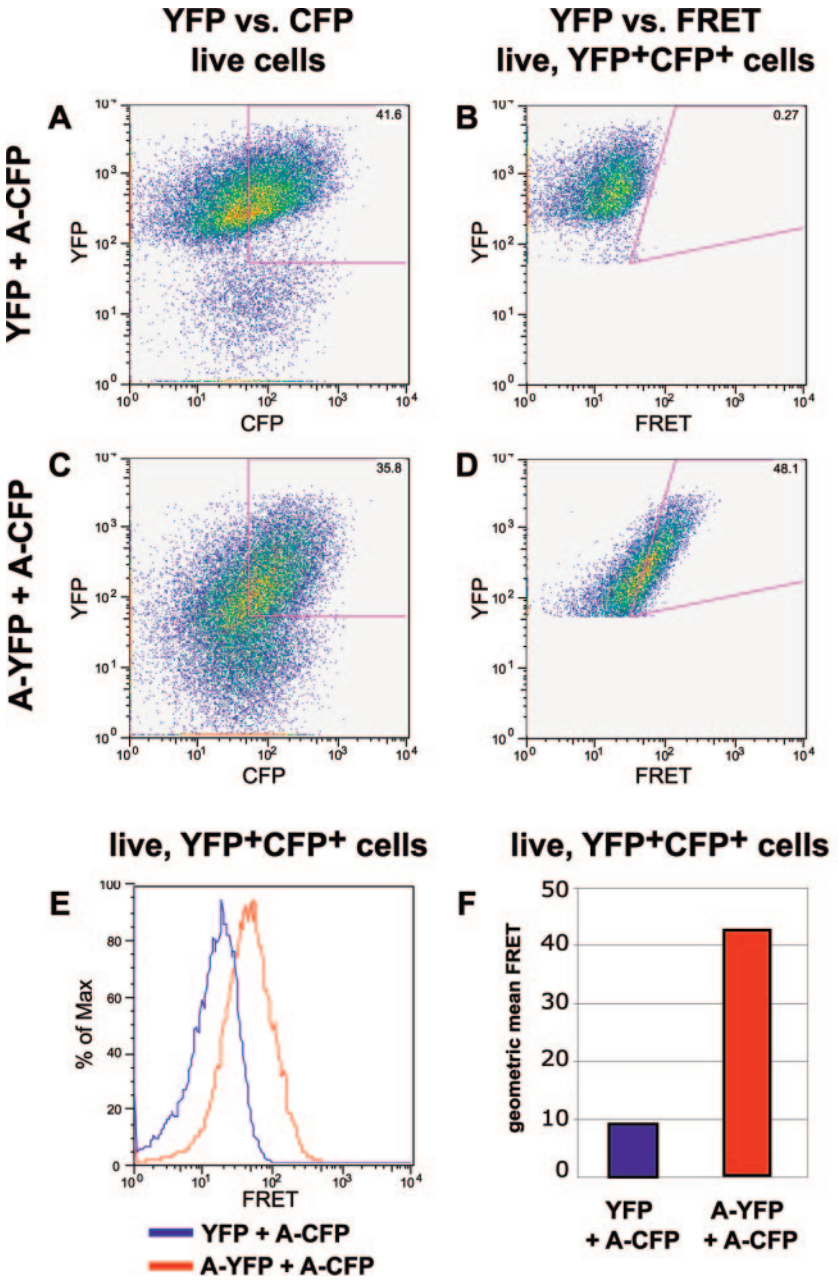

FIG. 2. Self-interaction of protein A as demonstrated by FRET. Yeast coexpressing either YFP and A-CFP (A and B) or A-YFP and A-CFP (C and D) were analyzed by flow cytometry, and data from live cells were plotted in logarithmic, pseudocolor dot plots of YFP fluorescence versus CFP fluorescence (A and C). Cells from each sample that coexpressed both YFP and CFP moieties were identified by the gate shown in panels A and C (YFP^+ CFP^+ gate; magenta box) and replotted in YFP versus FRET plots in panels B and D, respectively. The gate shown in panels B and D (FRET gate; magenta box) includes only the cells that displayed higher FRET intensities than the negative control (B). Numbers inside the gates indicate the percentages of cells in the parent population that fell into the gate. Colors in the dot plots indicate the density of points in a given area. Purple represents individual points and a low density of points. Blue, green, yellow, and red represent increasingly higher densities of points. The FRET channel intensities of live, YFP^+ CFP^+ cells from samples coexpressing either YFP and A-CFP (blue) or A-YFP and A-CFP (red) are shown in the log-scale histogram in panel E. The geometric means of the FRET channels depicted in panel E are plotted in panel F.

Due to plasmid loss (26), stochastic expression (53), and other factors, not every cell in a given sample will express both fluorescent fusion proteins. Since cells that do not express both the CFP fusion and the YFP fusion cannot possibly display FRET in our system, their removal eliminates potentially misleading data. Thus, only YFP^+ CFP^+ cells were considered in analyses of FRET. To examine the expression of the fluorescent proteins, flow cytometry data were graphed in log scale dot plots of the YFP fluorescence versus the CFP fluorescence of live cells coexpressing free YFP and A-CFP (Fig. 2A) or A-YFP and A-CFP (Fig. 2C). A gate for YFP^+ CFP^+ cells (magenta box, Fig. 2A and C) based on control samples ex-

pressing only A-YFP or only A-CFP identifies cells that exhibited both YFP and CFP fluorescence well above background. Based on this gate, ca. 42% of the live cells in the negative control sample expressed both YFP and A-CFP (Fig. 2A), and ca. 36% of the live cells in the experimental sample expressed both A-YFP and A-CFP (Fig. 2C).

To assess FRET, data from the YFP^+ CFP^+ cells gated in Fig. 2A and C were used to generate dot plots of YFP fluorescence versus FRET intensity, as shown in Fig. 2B and D, respectively. A FRET gate (magenta box, Fig. 2B and D) was drawn on the plot in Fig. 2B to identify that region on the graph into which only cells exhibiting higher FRET intensities than the negative control cells coexpressing YFP and A-CFP would fall. The bottom border of the FRET gate represents a threshold intensity in the YFP channel that was superceded only by cells that expressed YFP, and the left border of the gate represents a threshold FRET intensity that cells that coexpressed A-CFP and YFP failed to surpass. Whereas the FRET gate included only 0.3% of YFP^+ CFP^+ cells from the sample coexpressing YFP and A-CFP (Fig. 2B), 48% of YFP^+ CFP^+ cells from the experimental sample coexpressing A-YFP and A-CFP fell into the gate (Fig. 2D), indicating that FRET, and thus protein A-protein A interaction, occurred in these cells.

In addition, direct visual comparison of Fig. 2B and D shows that the cells from the experimental sample (Fig. 2D) exhibited overall higher fluorescence intensities in the FRET channel (*x* axis) than did cells from the negative control (Fig. 2B). This is further exemplified by the histogram in Fig. 2E depicting the FRET channels of these samples. Moreover, the geometric mean of the FRET channel from the experimental sample was 4.7-fold higher than that of the control (Fig. 2F). To ensure reproducibility, these and other FRET experiments described in the present study were repeated at least three times, and representative data are shown in the figures.

All of the comparisons made in Fig. 2 are valid means of determining that FRET occurred in the experimental sample since an appropriate negative control was used. However, gating holds an important advantage in that it reliably takes into consideration the variability of fusion protein expression and the effect that this variability has on FRET measurements (14). The FRET gate is derived from a two-dimensional plot such that it requires cells expressing higher levels of YFP to exhibit correspondingly higher FRET intensities in order to be considered FRET positive, thus adding stringency to the assay. In contrast, one-dimensional measurements such as the geometric mean FRET do not take the variability of fusion protein expression into account. Thus, gating analyses provide a more stringent, definitive, and comparative assessment of FRET. For these reasons, gating analyses were used to assess FRET in subsequent experiments (see below).

(ii) BRET. Green fluorescent protein (GFP) derivatives can dimerize, but only at very high concentrations (K_d = 110 μM) (76). Thus, the possibility that FRET was observed in Fig. 2 due to CFP/YFP-mediated dimerization rather than protein A self-interaction was remote. Nevertheless, to verify the significance of the FRET result and further confirm the self-interaction of protein A, we also performed a bioluminescence resonance energy transfer (BRET) assay. BRET is very similar to FRET, with the key difference that the light donor in BRET is a bioluminescent protein rather than a fluorescent protein (75). In the system we used, BRET occurs if the light energy produced by a fusion of *Renilla reniformis* luciferase to the C terminus of protein A (A-RL) is transferred to A-YFP. BRET is observed as the YFP fluorescence produced upon the addition of coelenterazine, a bioluminescent substrate of *Renilla* luciferase that yields light with an emission maximum of ~475 nm, similar to CFP. Like FRET, BRET occurs only when the fusion proteins are brought into extremely close proximity, typically achieved only by protein-protein interaction (75). Since *Renilla* luciferase does not interact with *Aequorea* GFP derivatives (75), BRET cannot be induced by their direct association and is therefore dependent on the interaction of the protein A sequences present in the fusions.

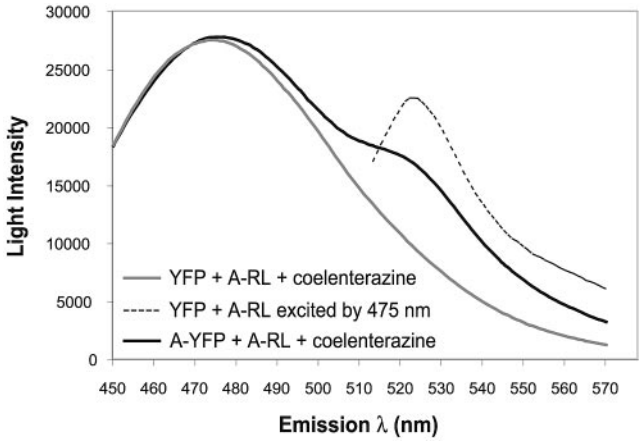

FIG. 3. Self-interaction of protein A as demonstrated by BRET. Coelenterazine was added to yeast cells coexpressing either YFP and A-RL (gray line) or A-YFP and A-RL (black line), and light emitted in the range of 450 to 570 nm wavelength was analyzed by spectrofluorometry in the absence of an excitation laser. For reference, YFP fluorescence was observed by exciting the sample coexpressing YFP and A-RL with a 475-nm laser prior to coelenterazine addition and monitoring emission over 515 to 570 nm wavelength (dashed line).

As a negative control, coelenterazine was added to a yeast culture coexpressing A-RL and free YFP (Fig. 3, gray line), and the emitted light was analyzed by spectrofluorometry. As expected, a single peak at ~475 nm was generated by luciferase bioluminescence, but no YFP fluorescence (emission at ~530 nm) was detectable unless the sample was directly excited by a 475-nm laser (Fig. 3, dashed line). In contrast, when coelenterazine was added to yeast cells coexpressing A-RL and A-YFP (Fig. 3, black line), two peaks were observed: the bioluminescence peak at ~475 nm and the YFP fluorescence peak at ~530 nm. The production of YFP fluorescence from *Renilla* luciferase bioluminescence thus indicates that BRET occurred between the A-RL and A-YFP fusions and that protein A self-interaction took place.

(iii) Coimmunoprecipitation. To further corroborate the FRET and BRET results and to test for interaction in insect cells that are fully susceptible to productive infection by FHV virions, we also performed coimmunoprecipitation in *Drosophila* cells (Fig. 4). *Drosophila* S2 cells were stably transfected with either empty vector (pMT/V5; lane 1), a plasmid expressing protein A with a C-terminal HA tag (pA-HA; lane 2), a plasmid expressing protein A with a C-terminal hexahistidine-

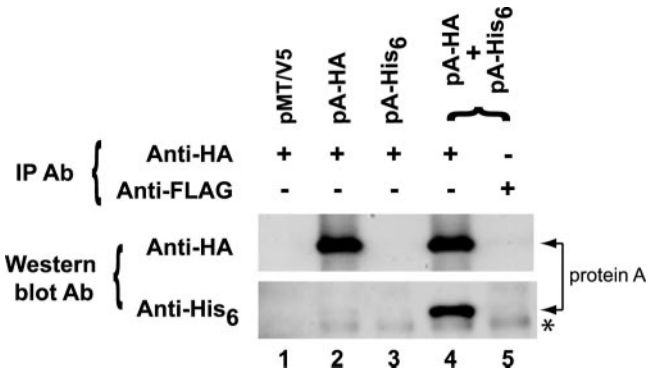

FIG. 4. Self-interaction of protein A as demonstrated by coimmunoprecipitation. *Drosophila* S2 cells were stably transfected with either empty vector (lane 1) or vectors expressing either HA-tagged protein A (lane 2), hexahistidine-tagged protein A (lane 3), or both (lanes 4 and 5). Lysates were immunoprecipitated with either an anti-HA antibody (lanes 1 to 4) or an anti-FLAG antibody (lane 5) and probed by Western blotting with either an anti-HA antibody (upper panel) or an anti-hexahistidine antibody (lower panel). Protein A is indicated by arrows, and an asterisk indicates the position of a nonspecific band.

tag (pA-His_6; lane 3), or with both pA-HA and pA-His_6 (lanes 4 to 5). After 24 h of induction, cells were harvested, and protein complexes were immunoprecipitated with an anti-HA antibody (lanes 1 to 4). The anti-HA antibody was specific to protein A-HA (lane 2), since it did not directly precipitate His_6-tagged protein A (lane 3). As expected, protein A-His_6 copurified with protein A-HA upon immunoprecipitation with the anti-HA antibody (lane 4), whereas neither protein was brought down with a control antibody (lane 5). Thus, protein-A self-interaction was also observed in insect cells by coimmunoprecipitation.

Identification of protein A sequences sufficient for protein-protein interaction. Protein A is a 998-amino-acid polypeptide containing an N-terminal transmembrane domain sufficient for localization to the outer mitochondrial membrane and a central region with homology to other RdRps (Fig. 5A) (38). To identify sequences in protein A that are sufficient to direct self-interaction, we included each of the indicated protein A fragments (Fig. 5A) in CFP and YFP fusion proteins. Each CFP-YFP pair of identically truncated fusion proteins was coexpressed in yeast cells and tested for homotypic protein-protein interaction by assaying FRET using flow cytometry. As before (Fig. 2) (14), FRET-positive cells were identified in gating analyses as cells exhibiting higher FRET intensities than negative controls. FRET gates for each CFP-YFP pair were adjusted to three negative control samples incapable of FRET: yeast cells expressing only the respective protein A-CFP fusion, yeast cells expressing only the respective protein A-YFP fusion, and yeast cells coexpressing the protein A-CFP fusion and free YFP.

Four of the fusion derivatives tested did not accumulate to levels detectable by flow cytometry and could not be assessed for FRET (Fig. 5A). Of the sequences that were expressed sufficiently, 10 did not exhibit FRET, and 13 displayed various degrees of FRET (Fig. 5A). Whereas all negative controls and FRET-negative samples contained less than 1% of YFP^+ CFP^+ cells in the FRET gate, FRET-positive samples contained 2.5% (amino acids 200 to 250 [aa 200-250]) to 52% (aa 200-300) of YFP^+ CFP^+ cells in the FRET gate. Selected data are also depicted in Fig. 5B, which shows the averages of at least three FRET mesurements for a subset of the protein A fragments in Fig. 5A. All FRET-positive samples reproducibly exhibited significantly higher FRET intensities than negative controls, indicating that the included sequences were sufficient to direct homotypic protein-protein interaction.

A series of FRET experiments with the N-terminal 200 amino acids of protein A (aa 1-200) and several N-terminal deletions (aa 200-998, 400-998, 600-998, 700-998, and 800-998) (Fig. 5A, top set of protein A fragments) suggested that sequences from at least two different regions of protein A (aa 1-200 and 200-800) were sufficient to support FRET. These sequences were further examined by testing the ability of smaller, overlapping segments of 100 amino acids (Fig. 5A, middle set of protein A fragments) to undergo FRET, revealing that the region spanning aa 700-800 and additional sequences in the region from aa 1-500 were sufficient for homotypic interaction. The region from 1-500 aa was further investigated by testing segments of 50 amino acids (Fig. 5A, bottom set of protein A fragments), two of which (aa 1-50 and aa 200-250) exhibited FRET. Thus, several protein A sequences were found to self interact. Two of these sequences (aa 1-200 and aa 200-300) produced high FRET signals that were near or surpassing that of wt protein A. Other interacting sequences produced weaker signals that were nevertheless significantly and reproducibly higher than negative controls. The various FRET intensities of these samples are considered further in the Discussion.

None of the partial protein A sequences tested in Fig. 5A were capable of producing FRET when they were expressed as YFP fusions and paired with a CFP fusion containing full-length protein A (A-CFP). A subset of these data are shown in Fig. 5B. Although one would predict that some of these fusion protein pairs would interact, it is not unreasonable that FRET was not observed in these experiments. FRET requires the YFP and CFP chromophores to be extremely close and precisely juxtaposed. Thus, although interaction may have occurred between a small YFP fusion and the larger, full-length CFP fusion, the chromophores may nevertheless be positioned improperly due to asymmetries in the size and geometry of the proteins. Furthermore, many of the sequences tested in Fig. 5A lack the N-terminal mitochondrial localization signal and thus would not colocalize with the full-length A-CFP fusion at the outer mitochondrial membrane. Even so, the absence of FRET between full-length and truncated protein A fusions underscores the stringency of this approach. The lack of FRET between the aa 1-200 YFP fusion and A-CFP, e.g., demonstrates that colocalization to the mitochondria is not sufficient to produce FRET and indicates that the dimerization of protein A fusion proteins is not driven by direct CFP-YFP interaction. In addition, when the CFP and YFP moieties of the full-length protein A fusions were mutated to prevent any possibility of CFP-YFP dimerization (L221K mutation; see reference 76), no effect on FRET was observed (not shown), further validating the dependence of FRET on protein A self-association. FRET is thus a rigorous indicator of protein-protein interaction, and false-positive observations of FRET are unlikely.

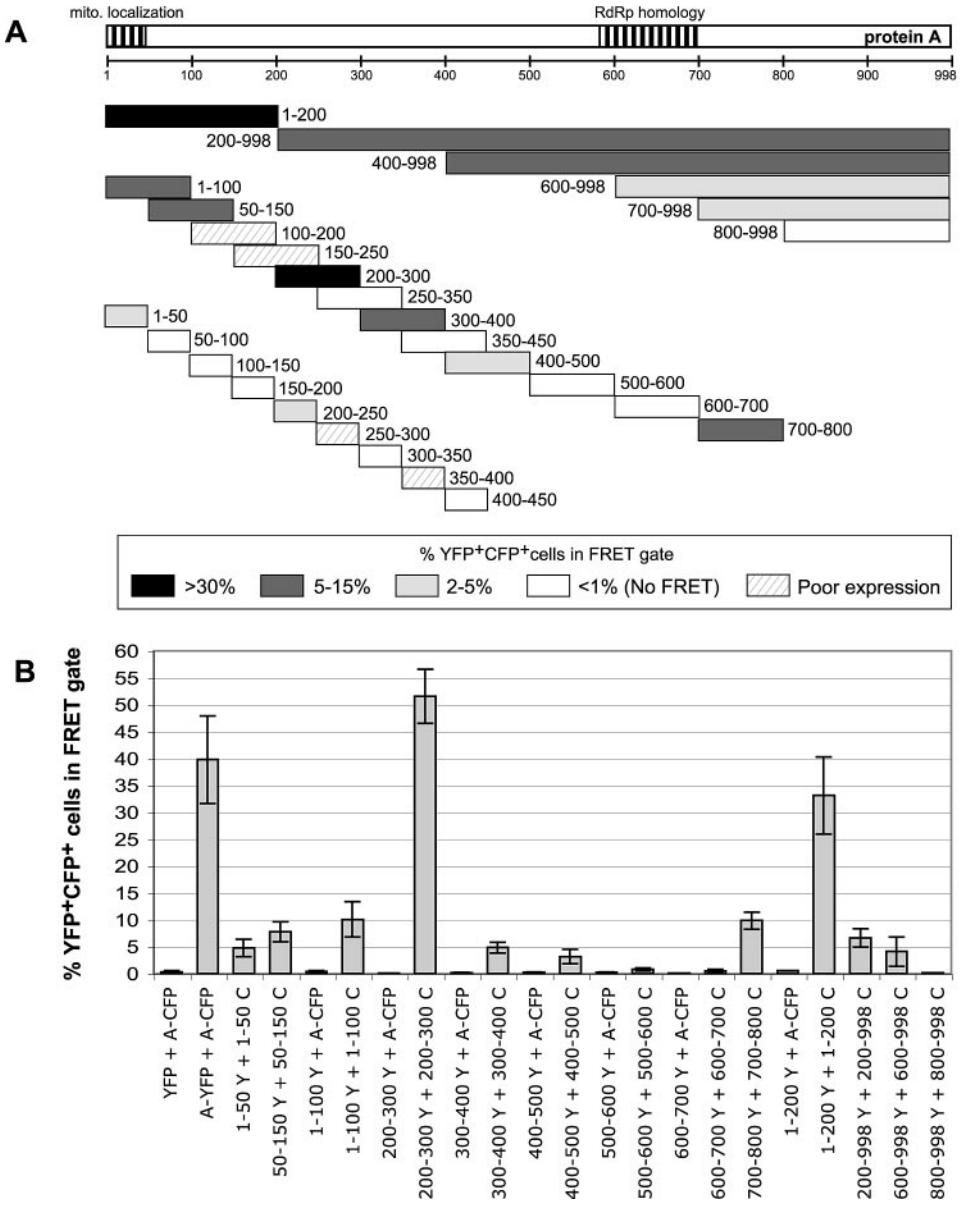

FIG. 5. Identification of protein A sequences sufficient to direct homotypic interaction. (A) Pairs of CFP and YFP fusion proteins were coexpressed in yeast cells and tested for FRET. Each fusion protein in a given CFP-YFP pair contained an identical protein A sequence. The protein A sequences tested in these assays are indicated by boxes; the numbers of the included amino acids are alongside each. The shading of the boxes corresponds to the percentage of live, YFP^+ CFP^+ cells from each sample that fell into the FRET gate, as denoted in the legend. Hatched boxes indicate sequences whose expression was too low for analysis. Each box is drawn to scale and aligned to a diagram of full-length protein A (top) to indicate the relative location of the sequence in the wt protein. Vertical stripes in the protein A schematic represent the mitochondrial localization domain and region of highest RdRp homology, as indicated. The number bar below the schematic denotes the positions of amino acids in protein A. The bar graph in B includes the results from a subset of the experiments in A and results from experiments in which the indicated YFP fusion was paired with the full-length A-CFP fusion. Error bars indicate ±1 standard deviation.

FRET also was used to test for heterotypic protein A-protein A interactions. Since multiple interaction domains were mapped to the N-terminal portion of protein A, a series of sequences spanning this region (aa 1-100, 200-300, 300-400, 400-500, and 500-600) were chosen for these studies. Protein A-CFP fusions containing these sequences were coexpressed in yeast in permuted combinations with their counterpart YFP fusions, and FRET was assessed by flow cytometry (Table 1). As shown previously, four of the five homotypic pairings of these sequences clearly produced FRET (Table 1 and Fig. 5). In addition, one heterotypic pairing (aa 300-400 + aa 400-500) also displayed FRET (4% of YFP^+ CFP^+ cells in the FRET gate), indicative of protein-protein interaction (Table 1). Whether this heterotypic interaction occurs as an intermolecular or intramolecular association in the context of the full-length protein remains unclear.

FRET correlates with RNA replication activity. To examine whether protein A self-interaction is relevant to its function,

TABLE 1. FRET analyses of homotypic and heterotypic interactions

CFP fusion	YFP fusion[a]				
	1–100	200–300	300–400	400–500	500–600
1–100	***10.1 ± 3.3***	0.6 ± 0.2	0.1 ± 0.1	0.7 ± 0.3	0.1 ± 0.1
200–300		***51.6 ± 5.0***	0.6 ± 0.3	0.8 ± 0.1	0.6 ± 0.2
300–400			***4.8 ± 1.0***	**4.3 ± 1.7**	0.3 ± 0.2
400–500				***3.2 ± 1.3***	0.9 ± 0.7
500–600					*0.8 ± 0.3*

[a] FRET was measured as the percentage of YFP^+ CFP^+ cells that fell into the FRET gate. The average of at least three experiments ± standard deviation is reported. Boldface numerals indicate pairings that were positive for FRET; homotypic pairings are italicized.

we tested the effects of protein A-YFP mutations on FRET and FHV RNA replication. Single amino acid substitutions in the full-length protein A-YFP fusion were introduced within a region spanning aa 203 to 247 because the fragment encoding aa 200-300 produced the strongest FRET signal observed (Fig. 5) and because the fragment encoding aa 200-250 was the smallest segment outside of a sequence containing the N-terminal mitochondrial localization domain (aa 1-50) shown to self-interact. In each mutant, the indicated amino acid was changed to alanine.

The effect of these mutations on FRET was tested by coexpressing each protein A-YFP mutant with wt A-CFP in yeast cells and performing flow cytometry analyses as described earlier. As shown in Fig. 6A and B, samples expressing wt A-YFP contained, on average, 40% of YFP^+ CFP^+ cells in the FRET gate. In contrast, four mutants (N203, W220, W222, and S231) exhibited marked reductions in FRET so that only 3 to 5% of YFP^+ CFP^+ cells from these samples fell into the FRET gate. Other mutations had lesser effects on FRET, with 22 to 40% of YFP^+ CFP^+ cells falling in the FRET gate.

To test the ability of these protein A derivatives to support FHV RNA replication, wt A-YFP and each mutant protein A-YFP fusion were separately expressed in yeast cells cotransformed with pFHV1-RL, a plasmid encoding an FHV replication reporter. pFHV1-RL expresses a modified form of FHV RNA1 that contains a frameshift mutation in the protein A ORF and an insertion of the *Renilla* luciferase ORF in the region encoding the subgenomic RNA3 (Fig. 6C). Since the protein A ORF is disrupted in this construct, replication of the RNA1 transcript from pFHV1-RL is dependent on the RdRp activity of the protein A-YFP fusion expressed in *trans* from a second plasmid (50, 51). Since RNA3 is produced only upon the protein A-dependent replication of RNA1, *Renilla* luciferase is expressed only if the protein A-YFP fusion provided in *trans* retains replication activity (50).

As shown in Fig. 6, wt A-YFP supported FHV replication, as demonstrated by the production of luciferase activity when coexpressed with pFHV1-RL. Strikingly, the YFP fusion mutants that exhibited large reductions in FRET (N203, W220, W222, and S231) displayed significant reductions in replication, retaining only 2 to 6% of the activity observed for wt A-YFP (Fig. 6A and B). Thus, a correlation was observed between the disruption of FRET and impaired replication. Three mutants that maintained relatively high levels of FRET (Y207, W215, and E227) also exhibited low replication activi-

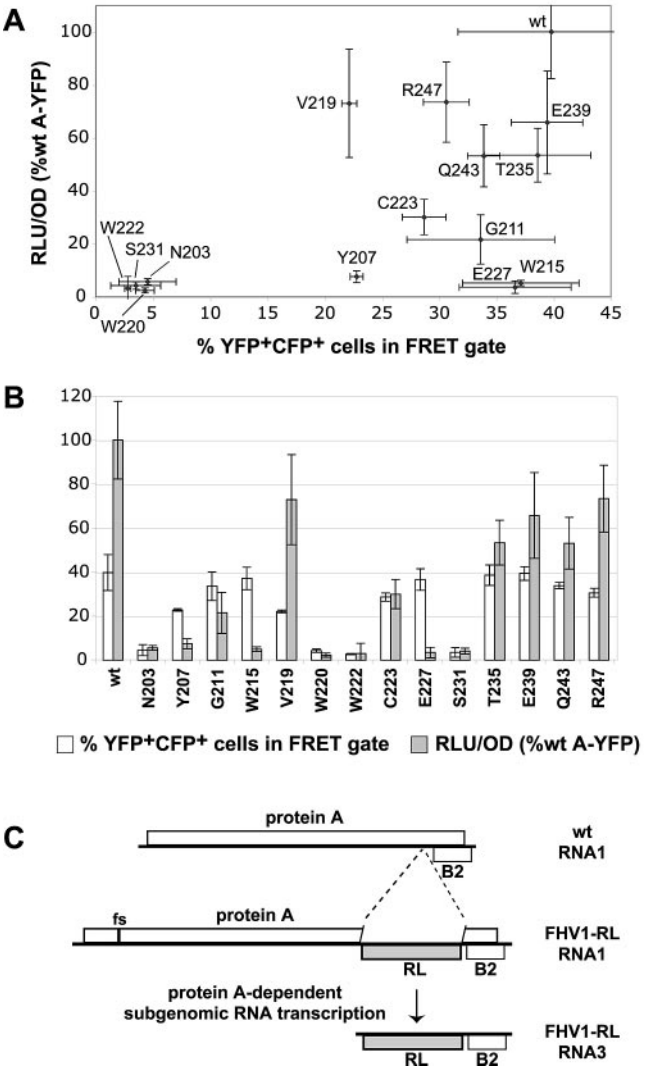

FIG. 6. FRET correlates with RNA replication activity. Protein A-YFP fusions in which the indicated amino acids were mutated to alanine were coexpressed in yeast cells with wt A-CFP, and FRET was analyzed by flow cytometry. The ability of each mutant to support FHV RNA replication was measured by using an in vivo reporter-based assay. The graph in panel A plots the RNA replication activity versus FRET for each of the indicated protein A-YFP mutants and for wild-type A-YFP (wt). For added clarity, these data are reiterated in the bar graph in panel B. Columns: □, FRET; ▨, RNA replication activity. (C) RNA replication was assayed by using an FHV RNA1 construct (pFHV1-RL) in which the *Renilla* luciferase (RL) ORF has been inserted into the region of FHV RNA1 that encodes subgenomic RNA3. A frameshift (fs) mutation in the protein A ORF of pFHV1-RL renders the expression of RL dependent on the replicase activity of a protein A-YFP fusion coexpressed from a second plasmid. RNA replication activity is reported as the percentage of luciferase activity produced by each protein A-YFP mutant relative to wt A-YFP when coexpressed in yeast cells with pFHV1-RL. Luciferase activity was measured as the relative light units (RLU) produced per optical density unit of yeast culture and was normalized to the expression level of each YFP fusion. FRET is reported as the percentage of live, YFP^+ CFP^+ cells that fell into the FRET gate. Error bars indicate ±1 standard deviation.

ties (8, 5, and 4% of wt A-YFP, respectively). These data do not contradict the correlation between FRET and replication since some mutations may affect other aspects of protein A function and thus replication, but not disrupt protein-protein interaction and FRET. Thus, large reductions in FRET were always accompanied by large reductions in replication activity, a finding consistent with a requirement for protein A self-interaction in RNA replication.

DISCUSSION

Protein A self-interaction. To test for possible self-interaction of protein A, we performed FRET (Fig. 2) and BRET (Fig. 3) experiments in yeast cells and coimmunoprecipitation experiments in *Drosophila* cells (Fig. 4). Each of these independent techniques indicated that protein A self-interacts in vivo, and their combined use provides a strong body of evidence for protein A self-association. In addition, the correlation between a reduction in FRET and the attenuation of replication activity implies that protein A self-interaction is important for its function (Fig. 6).

Proteins fused to GFP derivatives often maintain activity (71), allowing in vivo CFP/YFP FRET analyses to be performed with functional proteins at their native sites of subcellular localization. Indeed, protein A-YFP retains replication activity (Fig. 6) and is localized to mitochondria, as evidenced by colocalization with a mitochondrion-specific dye, mitotracker red (Invitrogen) (results not shown). Thus, the FRET experiments observed steady-state self-interaction of functional protein A in live cells.

Similarly, BRET experiments were also performed in vivo and corroborated the FRET results. BRET confirmed that energy transfer was observed due to protein A-dependent interaction of the fusion proteins rather than the unlikely possibility of direct CFP-YFP dimerization. Coimmunoprecipitation further substantiated the FRET and BRET results via a biochemical approach and provided evidence for protein A self-interaction in an insect host.

Multiple self-interaction domains in protein A and other viral replicase proteins. To further characterize protein A self-interaction, we tested the ability of truncated protein A fusions to produce FRET. These experiments identified sequences spanning six nonoverlapping regions (aa 1-50, 50-150, 200-300, 300-400, 400-500, and 700-800) that were sufficient to promote homotypic protein-protein interactions (Fig. 5). The intensity of FRET produced by these interactions varied. Some of these had relatively low FRET responses, with <5% of YFP^+ CFP^+ cells in the FRET gate (aa 1-50, 200-250, 400-500, 600-998, and 700-998). In other cases (aa 1-100, 50-150, 300-400, 700-800, 200-998, and 400-998), between 5 and 15% of YFP^+ CFP^+ cells fell in the FRET gate. Strikingly, however, two segments (aa 1-200 and 200-300) displayed high FRET signals in which 33 and 52%, respectively, of YFP^+ CFP^+ cells fell into the FRET gate, a finding comparable to that for full-length protein A. High FRET signals are indicative of substantial interactions between fusion proteins. However, low FRET signals can result from suboptimal chromophore geometries even if the fusion proteins form strong interactions. Nevertheless, it is still likely that the fusions that yielded the highest FRET measurements (aa 1-200 and 200-300) also produced the strongest interactions and contain the sequences most important in protein A self-association. In addition, subsets of each of these sequences (aa 1-50, 1-100, 50-150, and 200-250) were shown to produce FRET, corroborating the self-interaction of both the aa 1-200 and 200-300 regions.

Replicase proteins from other positive-strand RNA viruses have also been shown to form multiple protein-protein interactions. The 3D polymerase of poliovirus was shown to homo-oligomerize via two interfaces, and mutation of these sequences resulted in the loss of RNA binding, prevented the extension of RNA templates, and disrupted the formation of higher-order polymerase structures (24, 37). Brome mosaic virus (BMV) and tobacco mosaic virus (TMV) each encode two replicase proteins. BMV encodes 1a, which contains capping and helicase domains, and 2a, which contains an RdRp domain (1, 29). 1a localizes to endoplasmic reticulum membranes and induces membrane invaginations that serve as compartments for BMV RNA replication and show strikingly similar morphology to the mitochondrial spherules associated with FHV RNA replication (39, 65). TMV expresses a 126-kDa protein that shares striking similarities in sequence, expression, and function to 1a (2, 25) and a 183-kDa protein analogous to 2a produced by readthrough translation of the 126-kDa ORF (49). Both 1a and the 126-kDa protein form interactions with their respective 2a and 183-kDa counterparts (21, 22, 41, 42). In addition, both N-terminal/N-terminal and N-terminal/C-terminal self-interactions have been described for 1a (41, 42), and more recent work has found that self-interaction of the 126-kDa protein helicase domain can direct the formation of hexamer-like oligomers (21, 22).

Multiple interaction domains are also found in retroviral Gag and Gag-Pol proteins, whose well-studied assembly of virion cores appears to have similarities to the formation of BMV RNA replication spherules (65). The I domain of human immunodeficiency virus type 1 Gag, located within the nucleocapsid domain, appears to be the primary sequence responsible for Gag-Gag dimerization (13, 57). However, the matrix and capsid domains also contribute to gag interactions (10; reviewed in reference 20), and the reverse transcriptase domain present in gag-pol can also direct dimerization (55, 68, 73). Furthermore, the matrix, capsid, and nucleocapsid domains are located N-terminal relative to the reverse transcriptase domain of Gag-Pol (20), paralleling FHV protein A, in which interaction sites were found primarily upstream of the RdRp motif (Fig. 5).

The presence of multiple putative interaction domains raises several potential models for the mechanism of protein A interaction. It is possible that all of these contacts form simultaneously such that two protein A molecules in a dimer contact one another at multiple interfaces. If protein A forms higher-order oligomers, multiple protein A molecules could interact such that each molecule contacts another using a different interaction domain. Alternatively, some interaction interfaces, conformations, or multimer states may be specific to certain protein A functions. For example, different contacts may mediate distinct interactions, or different protein A conformers, in successive steps such as replication complex assembly, negative-strand RNA synthesis, positive-strand RNA synthesis, and RNA capping. The observation of a heterotypic protein A interaction (Table 1) is also consistent with possible modula-

tions of protein A self-interactions during the viral life cycle. Since the segments of protein A from aa 300-400 and aa 400-500 were found to interact both with themselves and with each another, competition between the heterotypic and homotypic interactions may exist and serve to alter the structure, multimerization, or function of protein A. In any case, results from FRET, BRET, and coimmunoprecipitation experiments demonstrate protein A self-association (Fig. 2 to 4), and deletion analyses reveal that multiple protein A sequences are capable of directing protein-protein interaction (Fig. 5 and Table 1).

Correlation of protein A interaction with RNA replication. The point mutants shown in Fig. 6 differ from wt protein A-YFP by only a single amino acid. Therefore, it is likely that a reduced level of FRET between a mutant protein A-YFP fusion and wt A-CFP is due to a genuine perturbation of protein-protein interaction rather than an aberrant juxtaposition of chromophores. In either case, a significant reduction in FRET caused by the introduction of a point mutation reflects an alteration in the physical interaction between protein A fusions. Regardless of whether these mutations diminished FRET by weakening protein A-protein A interaction or by altering the geometry of the interaction to weaken only FRET, they nevertheless led to a change in protein A self-association that also disrupted RNA replication. Thus, the observed correlation between diminished FRET and a reduction in replication activity (Fig. 6) signifies that the fidelity of protein A self-association is important for its function.

In summary, the observations presented here are consistent with a model in which protein A functions as a multimer during several different steps of FHV RNA replication, from spherule formation to RNA synthesis. Experiments can now be designed to address the role of protein A self-interaction at specific steps in the replication pathway. As discussed above, the multimerization of protein A and its importance in RNA replication activity parallels recent observations made for the replicase proteins of other RNA viruses, suggesting that the self-interaction of replication factors is a common feature of positive-strand RNA viruses. In addition, the present study further demonstrates the advantages of flow cytometric FRET analysis in observing in vivo protein-protein interactions.

ACKNOWLEDGMENTS

We thank K. Schell, J. Puchalski, and J. Batchelder at the University of Wisconsin Comprehensive Cancer Center Flow Cytometry Facility for assistance with flow cytometry data collection. Spectrofluorometry data for BRET experiments were obtained at the University of Wisconsin-Madison Biophysics Instrument Facility, established with funding from the University of Wisconsin, NSF (BIR-9512577), and NIH (S10 RR13790). We thank B. Lindenbach for pFHV1-RL.

This research was supported by NIH grant GM35072. P.A. is an investigator of the Howard Hughes Medical Institute.

REFERENCES

1. **Ahlquist, P.** 1992. Bromovirus RNA replication and transcription. Curr. Opin. Genet. Dev. **2:**71–76.
2. **Ahlquist, P., E. G. Strauss, C. M. Rice, J. H. Strauss, J. Haseloff, and D. Zimmern.** 1985. Sindbis virus proteins nsP1 and nsP2 contain homology to nonstructural proteins from several RNA plant viruses. J. Virol. **53:**536–542.
3. **Albarino, C. G., L. D. Eckerle, and L. A. Ball.** 2003. The *cis*-acting replication signal at the 3′ end of flock house virus RNA2 is RNA3-dependent. Virology **311:**181–191.
4. **Andino, R., G. E. Rieckhof, P. L. Achacoso, and D. Baltimore.** 1993. Poliovirus RNA synthesis utilizes an RNP complex formed around the 5′-end of viral RNA. EMBO J. **12:**3587–3598.
5. **Arnold, J. J., and C. E. Cameron.** 1999. Poliovirus RNA-dependent RNA polymerase (3Dpol) is sufficient for template switching in vitro. J. Biol. Chem. **274:**2706–2716.
6. **Ball, L. A.** 1992. Cellular expression of a functional nodavirus RNA replicon from vaccinia virus vectors. J. Virol. **66:**2335–2345.
7. **Ball, L. A.** 1995. Requirements for the self-directed replication of flock house virus RNA 1. J. Virol. **69:**720–727.
8. **Ball, L. A., and K. L. Johnson.** 1998. Nodaviruses of insects, p. 225–267. *In* L. K. Miller and L. A. Ball (ed.), The insect viruses. Plenum Publishing Corp., New York, N.Y.
9. **Beckman, M. T., and K. Kirkegaard.** 1998. Site size of cooperative single-stranded RNA binding by poliovirus RNA-dependent RNA polymerase. J. Biol. Chem. **273:**6724–6730.
10. **Burniston, M. T., A. Cimarelli, J. Colgan, S. P. Curtis, and J. Luban.** 1999. Human immunodeficiency virus type 1 Gag polyprotein multimerization requires the nucleocapsid domain and RNA and is promoted by the capsid-dimer interface and the basic region of matrix protein. J. Virol. **73:**8527–8540.
11. **Dasgupta, R., L. L. Cheng, L. C. Bartholomay, and B. M. Christensen.** 2003. Flock house virus replicates and expresses green fluorescent protein in mosquitoes. J. Gen. Virol. **84:**1789–1797.
12. **Dasgupta, R., B. Selling, and R. Rueckert.** 1994. Flock house virus: a simple model for studying persistent infection in cultured *Drosophila* cells. Arch. Virol. **1994**(Suppl. 9)**:**121–132.
13. **Derdowski, A., L. Ding, and P. Spearman.** 2004. A novel fluorescence resonance energy transfer assay demonstrates that the human immunodeficiency virus type 1 Pr55Gag I domain mediates Gag-Gag interactions. J. Virol. **78:**1230–1242.
14. **Dye, B. T., K. Schell, D. J. Miller, and P. Ahlquist.** 2005. Detecting protein-protein interaction in live yeast by flow cytometry. Cytometry **63:**77–86.
15. **Eckerle, L. D., C. G. Albarino, and L. A. Ball.** 2003. Flock House virus subgenomic RNA3 is replicated and its replication correlates with transactivation of RNA2. Virology **317:**95–108.
16. **Eckerle, L. D., and L. A. Ball.** 2002. Replication of the RNA segments of a bipartite viral genome is coordinated by a transactivating subgenomic RNA. Virology **296:**165–176.
17. **Elble, R.** 1992. A simple and efficient procedure for transformation of yeasts. BioTechniques **13:**18–20.
18. **Fisher, A. J., B. R. McKinney, A. Schneemann, R. R. Rueckert, and J. E. Johnson.** 1993. Crystallization of viruslike particles assembled from flock house virus coat protein expressed in a baculovirus system. J. Virol. **67:**2950–2953.
19. **Förster, T.** 1965. Delocalized excitation and excitation transfer, p. 93–137. *In* O. Sinanoglu (ed.), Modern quantum chemistry, vol. 3. Academic Press, Inc., New York, N.Y.
20. **Freed, E. O.** 1998. HIV-1 gag proteins: diverse functions in the virus life cycle. Virology **251:**1–15.
21. **Goregaoker, S. P., and J. N. Culver.** 2003. Oligomerization and activity of the helicase domain of the tobacco mosaic virus 126- and 183-kilodalton replicase proteins. J. Virol. **77:**3549–3556.
22. **Goregaoker, S. P., D. J. Lewandowski, and J. N. Culver.** 2001. Identification and functional analysis of an interaction between domains of the 126/183-kDa replicase-associated proteins of tobacco mosaic virus. Virology **282:**320–328.
23. **Hancock, J. F.** 2003. Ras proteins: different signals from different locations. Nat. Rev. Mol. Cell. Biol. **4:**373–384.
24. **Hansen, J. L., A. M. Long, and S. C. Schultz.** 1997. Structure of the RNA-dependent RNA polymerase of poliovirus. Structure **5:**1109–1122.
25. **Haseloff, J., P. Goelet, D. Zimmern, P. Ahlquist, R. Dasgupta, and P. Kaesberg.** 1984. Striking similarities in amino acid sequence among nonstructural proteins encoded by RNA viruses that have dissimilar genomic organization. Proc. Natl. Acad. Sci. USA **81:**4358–4362.
26. **Ishikawa, M., M. Janda, M. A. Krol, and P. Ahlquist.** 1997. In vivo DNA expression of functional brome mosaic virus RNA replicons in *Saccharomyces cerevisiae*. J. Virol. **71:**7781–7790.
27. **Johnson, K. L., and L. A. Ball.** 1999. Induction and maintenance of autonomous flock house virus RNA1 replication. J. Virol. **73:**7933–7942.
28. **Johnson, K. L., and L. A. Ball.** 1997. Replication of flock house virus RNAs from primary transcripts made in cells by RNA polymerase II. J. Virol. **71:**3323–3327.
29. **Kao, C. C., and K. Sivakumaran.** 2000. Brome mosaic virus, good for an RNA virologist's basic needs. Mol. Plant Pathol. **1:**91–97.
30. **Krishna, N. K., D. Marshall, and A. Schneemann.** 2003. Analysis of RNA packaging in wild-type and mosaic protein capsids of flock house virus using recombinant baculovirus vectors. Virology **305:**10–24.
31. **Kujala, P., A. Ikaheimonen, N. Ehsani, H. Vihinen, P. Auvinen, and L. Kaariainen.** 2001. Biogenesis of the Semliki Forest virus RNA replication complex. J. Virol. **75:**3873–3884.
32. **Lewandowski, D. J., and W. O. Dawson.** 2000. Functions of the 126- and 183-kDa proteins of tobacco mosaic virus. Virology **271:**90–98.
33. **Li, H., W. X. Li, and S. W. Ding.** 2002. Induction and suppression of RNA silencing by an animal virus. Science **296:**1319–1321.

34. **Lindenbach, B. D., J. Y. Sgro, and P. Ahlquist.** 2002. Long-distance base pairing in flock house virus RNA1 regulates subgenomic RNA3 synthesis and RNA2 replication. J. Virol. **76:**3905–3919.
35. **Lohmann, V., F. Korner, U. Herian, and R. Bartenschlager.** 1997. Biochemical properties of hepatitis C virus NS5B RNA-dependent RNA polymerase and identification of amino acid sequence motifs essential for enzymatic activity. J. Virol. **71:**8416–8428.
36. **Lohmann, V., A. Roos, F. Korner, J. O. Koch, and R. Bartenschlager.** 1998. Biochemical and kinetic analyses of NS5B RNA-dependent RNA polymerase of the hepatitis C virus. Virology **249:**108–118.
37. **Lyle, J. M., E. Bullitt, K. Bienz, and K. Kirkegaard.** 2002. Visualization and functional analysis of RNA-dependent RNA polymerase lattices. Science **296:**2218–2222.
38. **Miller, D. J., and P. Ahlquist.** 2002. Flock house virus RNA polymerase is a transmembrane protein with amino-terminal sequences sufficient for mitochondrial localization and membrane insertion. J. Virol. **76:**9856–9867.
39. **Miller, D. J., M. D. Schwartz, and P. Ahlquist.** 2001. Flock house virus RNA replicates on outer mitochondrial membranes in *Drosophila* cells. J. Virol. **75:**11664–11676.
40. **Miller, D. J., M. D. Schwartz, B. T. Dye, and P. Ahlquist.** 2003. Engineered retargeting of viral RNA replication complexes to an alternative intracellular membrane. J. Virol. **77:**12193–12202.
41. **O'Reilly, E. K., J. D. Paul, and C. C. Kao.** 1997. Analysis of the interaction of viral RNA replication proteins by using the yeast two-hybrid assay. J. Virol. **71:**7526–7532.
42. **O'Reilly, E. K., Z. Wang, R. French, and C. C. Kao.** 1998. Interactions between the structural domains of the RNA replication proteins of plant-infecting RNA viruses. J. Virol. **72:**7160–7169.
43. **Palmenberg, A. C.** 1990. Proteolytic processing of picornaviral polyprotein. Annu. Rev. Microbiol. **44:**603–623.
44. **Panaviene, Z., J. M. Baker, and P. D. Nagy.** 2003. The overlapping RNA-binding domains of p33 and p92 replicase proteins are essential for tombusvirus replication. Virology **308:**191–205.
45. **Panaviene, Z., T. Panavas, S. Serva, and P. D. Nagy.** 2004. Purification of the cucumber necrosis virus replicase from yeast cells: role of coexpressed viral RNA in stimulation of replicase activity. J. Virol. **78:**8254–8263.
46. **Pata, J. D., S. C. Schultz, and K. Kirkegaard.** 1995. Functional oligomerization of poliovirus RNA-dependent RNA polymerase. RNA **1:**466–477.
47. **Patterson, G. H., D. W. Piston, and B. G. Barisas.** 2000. Förster distances between green fluorescent protein pairs. Anal. Biochem. **284:**438–440.
48. **Pawlotsky, J. M., and G. Germanidis.** 1999. The nonstructural 5A protein of hepatitis C virus. J. Viral Hepat. **6:**343–356.
49. **Pelham, H. R.** 1978. Leaky UAG termination codon in tobacco mosaic virus RNA. Nature **272:**469–471.
50. **Price, B. D., M. Roeder, and P. Ahlquist.** 2000. DNA-Directed expression of functional flock house virus RNA1 derivatives in *Saccharomyces cerevisiae*, heterologous gene expression, and selective effects on subgenomic mRNA synthesis. J. Virol. **74:**11724–11733.
51. **Price, B. D., R. R. Rueckert, and P. Ahlquist.** 1996. Complete replication of an animal virus and maintenance of expression vectors derived from it in *Saccharomyces cerevisiae*. Proc. Natl. Acad. Sci. USA **93:**9465–9470.
52. **Qin, W., H. Luo, T. Nomura, N. Hayashi, T. Yamashita, and S. Murakami.** 2002. Oligomeric interaction of hepatitis C virus NS5B is critical for catalytic activity of RNA-dependent RNA polymerase. J. Biol. Chem. **277:**2132–2137.
53. **Raser, J. M., and E. K. O'Shea.** 2004. Control of stochasticity in eukaryotic gene expression. Science **304:**1811–1814.
54. **Reed, K. E., and C. M. Rice.** 2000. Overview of hepatitis C virus genome structure, polyprotein processing, and protein properties. Curr. Top. Microbiol. Immunol. **242:**55–84.
55. **Restle, T., B. Muller, and R. S. Goody.** 1990. Dimerization of human immunodeficiency virus type 1 reverse transcriptase. A target for chemotherapeutic intervention. J. Biol. Chem. **265:**8986–8988.
56. **Russo, M., J. Burgyan, and G. P. Martelli.** 1994. Molecular biology of tombusviridae. Adv. Virus Res. **44:**381–428.
57. **Sandefur, S., R. M. Smith, V. Varthakavi, and P. Spearman.** 2000. Mapping and characterization of the N-terminal I domain of human immunodeficiency virus type 1 Pr55(Gag). J. Virol. **74:**7238–7249.
58. **Schaad, M. C., P. E. Jensen, and J. C. Carrington.** 1997. Formation of plant RNA virus replication complexes on membranes: role of an endoplasmic reticulum-targeted viral protein. EMBO J. **16:**4049–4059.
59. **Schlegel, A., T. H. Giddings, Jr., M. S. Ladinsky, and K. Kirkegaard.** 1996. Cellular origin and ultrastructure of membranes induced during poliovirus infection. J. Virol. **70:**6576–6588.
60. **Schmidt-Mende, J., E. Bieck, T. Hugle, F. Penin, C. M. Rice, H. E. Blum, and D. Moradpour.** 2001. Determinants for membrane association of the hepatitis C virus RNA-dependent RNA polymerase. J. Biol. Chem. **276:**44052–44063.
61. **Schneemann, A., R. Dasgupta, J. E. Johnson, and R. R. Rueckert.** 1993. Use of recombinant baculoviruses in synthesis of morphologically distinct virus-like particles of flock house virus, a nodavirus. J. Virol. **67:**2756–2763.
62. **Schneemann, A., T. M. Gallagher, and R. R. Rueckert.** 1994. Reconstitution of Flock House provirions: a model system for studying structure and assembly. J. Virol. **68:**4547–4556.
63. **Schneemann, A., and D. Marshall.** 1998. Specific encapsidation of nodavirus RNAs is mediated through the C terminus of capsid precursor protein alpha. J. Virol. **72:**8738–8746.
64. **Schneemann, A., W. Zhong, T. M. Gallagher, and R. R. Rueckert.** 1992. Maturation cleavage required for infectivity of a nodavirus. J. Virol. **66:**6728–6734.
65. **Schwartz, M., J. Chen, M. Janda, M. Sullivan, J. den Boon, and P. Ahlquist.** 2002. A positive-strand RNA virus replication complex parallels form and function of retrovirus capsids. Mol. Cell **9:**505–514.
66. **Scotti, P. D., S. Dearing, and D. W. Mossop.** 1983. Flock house virus: a nodavirus isolated from *Costelytra zealandica* (White) (Coleoptera: Scarabaeidae). Arch. Virol. **75:**181–189.
67. **Selling, B. H., R. F. Allison, and P. Kaesberg.** 1990. Genomic RNA of an insect virus directs synthesis of infectious virions in plants. Proc. Natl. Acad. Sci. USA **87:**434–438.
68. **Tachedjian, G., H. E. Aronson, M. de los Santos, J. Seehra, J. M. McCoy, and S. P. Goff.** 2003. Role of residues in the tryptophan repeat motif for HIV-1 reverse transcriptase dimerization. J. Mol. Biol. **326:**381–396.
69. **Tihova, M., K. A. Dryden, T. V. Le, S. C. Harvey, J. E. Johnson, M. Yeager, and A. Schneemann.** 2004. Nodavirus coat protein imposes dodecahedral RNA structure independent of nucleotide sequence and length. J. Virol. **78:**2897–2905.
70. **Truong, K., and M. Ikura.** 2001. The use of FRET imaging microscopy to detect protein-protein interactions and protein conformational changes in vivo. Curr. Opin. Struct. Biol. **11:**573–578.
71. **Tsien, R. Y.** 1998. The green fluorescent protein. Annu. Rev. Biochem. **67:**509–544.
72. **Van Der Heijden, M. W., J. E. Carette, P. J. Reinhoud, A. Haegi, and J. F. Bol.** 2001. Alfalfa mosaic virus replicase proteins P1 and P2 interact and colocalize at the vacuolar membrane. J. Virol. **75:**1879–1887.
73. **Wang, J., S. J. Smerdon, J. Jager, L. A. Kohlstaedt, P. A. Rice, J. M. Friedman, and T. A. Steitz.** 1994. Structural basis of asymmetry in the human immunodeficiency virus type 1 reverse transcriptase heterodimer. Proc. Natl. Acad. Sci. USA **91:**7242–7246.
74. **Wang, Q. M., M. A. Hockman, K. Staschke, R. B. Johnson, K. A. Case, J. Lu, S. Parsons, F. Zhang, R. Rathnachalam, K. Kirkegaard, and J. M. Colacino.** 2002. Oligomerization and cooperative RNA synthesis activity of hepatitis C virus RNA-dependent RNA polymerase. J. Virol. **76:**3865–3872.
75. **Xu, Y., A. Kanauchi, A. G. von Arnim, D. W. Piston, and C. H. Johnson.** 2003. Bioluminescence resonance energy transfer: monitoring protein-protein interactions in living cells. Methods Enzymol. **360:**289–301.
76. **Zacharias, D. A., J. D. Violin, A. C. Newton, and R. Y. Tsien.** 2002. Partitioning of lipid-modified monomeric GFPs into membrane microdomains of live cells. Science **296:**913–916.
77. **Zhong, W., R. Dasgupta, and R. Rueckert.** 1992. Evidence that the packaging signal for nodaviral RNA2 is a bulged stem-loop. Proc. Natl. Acad. Sci. USA **89:**11146–11150.
78. **Zhong, W., and R. R. Rueckert.** 1993. Flock house virus: down-regulation of subgenomic RNA3 synthesis does not involve coat protein and is targeted to synthesis of its positive strand. J. Virol. **67:**2716–2722.